

The non-rhombohedral low-temperature structure of PMN–10% PT

This article has been downloaded from IOPscience. Please scroll down to see the full text article.

2004 J. Phys.: Condens. Matter 16 7113

(<http://iopscience.iop.org/0953-8984/16/39/042>)

View [the table of contents for this issue](#), or go to the [journal homepage](#) for more

Download details:

IP Address: 129.252.86.83

The article was downloaded on 27/05/2010 at 18:00

Please note that [terms and conditions apply](#).

The non-rhombohedral low-temperature structure of PMN–10% PT

P M Gehring¹, W Chen², Z-G Ye² and G Shirane³

¹ NIST Center for Neutron Research, National Institute of Standards and Technology, Gaithersburg, MD 20899-8562, USA

² Department of Chemistry, Simon Fraser University, Burnaby, BC V5A 1S6, Canada

³ Physics Department, Brookhaven National Laboratory, Upton, NY 11973-5000, USA

Received 16 February 2004

Published 17 September 2004

Online at stacks.iop.org/JPhysCM/16/7113

doi:10.1088/0953-8984/16/39/042

Abstract

The phase diagram of the $\text{Pb}(\text{Mg}_{1/3}\text{Nb}_{2/3})\text{O}_3$ and PbTiO_3 solid solution (PMN– x PT) depicts a boundary between cubic and rhombohedral phases for $x \leq 0.32$. X-ray powder measurements reported by Dkhil *et al* show a rhombohedrally split (222) Bragg peak for PMN–10% PT at 80 K that is consistent with this phase boundary. Remarkably, our neutron data taken on a single crystal of the same compound with comparable q -resolution reveal a single resolution-limited (111) peak down to 50 K, and thus no rhombohedral distortion. Given the marked difference in penetration depths between x-rays and neutrons in these lead-oxide relaxor materials, our results suggest that the bulk structure, which is nearly cubic, differs from that of the outer layer in PMN–10% PT, a situation that has also recently been observed in PZN by Xu *et al*.

(Some figures in this article are in colour only in the electronic version.)

1. Introduction

The well-known relaxor $\text{Pb}(\text{Mg}_{1/3}\text{Nb}_{2/3})\text{O}_3$ (PMN) retains an average cubic structure down to 5 K when cooled in zero field (ZFC) [1–3]. In this respect PMN represents a puzzling anomaly among the complex-perovskite relaxors PMN– x PT and PZN– x PT ($M = \text{Mg}$, $Z = \text{Zn}$, $\text{PT} = \text{PbTiO}_3$, $0 \leq x \leq 1$) because all other compounds in these two systems that have been studied have been reported to exhibit a transition to a low temperature rhombohedral phase at low PT concentrations [4–7]. X-ray scattering measurements on a series of PMN– x PT compounds performed by Ye and coworkers, for example, demonstrate the presence of a clear rhombohedral distortion for PT concentrations as low as $x = 0.05$ [8] and with zero-field transition temperatures T_c that extrapolate to a non-zero value (210 K) at $x = 0$ (PMN). Similarly, Lebon *et al* [9] have reported a detailed x-ray study of the cubic-to-rhombohedral phase transition in single crystal PZN. An interesting comparison between PMN and PMN–10% PT was performed by Dkhil *et al* [10] using both x-ray and

neutron scattering methods on powder and single crystal samples that indicates the presence of competing tetragonal and rhombohedral order. In PMN, this never results in a ferroelectric distortion, but in PMN–10% PT a rhombohedral distortion was observed below a critical temperature $T_c = 285$ K. From these studies, PMN appears to be the exception in which a ferroelectric phase is never established.

Recent results, however, have begun to point towards a radically different physical picture. Neutron scattering data obtained by Ohwada *et al* [11] on a single crystal of PZN–8% PT suggest the presence of a low-temperature phase in the PZN– x PT system that is not rhombohedral, but instead has an average cubic structure. This new phase was termed ‘Phase X’. Striking evidence for this new phase was subsequently discovered by Xu *et al* [12] in single crystal PZN, where both the previously reported rhombohedral phase and Phase X were observed. More intriguing is the fact that the visibility of each phase depends on the x-ray energy, and thus on the x-ray penetration depth. At moderate x-ray energies (30 keV) Xu *et al* clearly observed a rhombohedral phase. However, at a much higher energy (67 keV) only a sharp unsplit (111) Bragg peak is seen, consistent with an average cubic structure.

In this paper, we report the results of an exceptionally high q -resolution neutron scattering study of a single crystal PMN–10% PT sample that traces the evolution of the (111) Bragg peak from the cubic phase well above $T_c = 285$ K down to 50 K. In stark contrast to the findings of Dkhil *et al* we observe no splitting of the (111) peak at any temperature as expected under a rhombohedral transformation. Instead, the (111) peak is nearly resolution-limited at low temperature, and comparable in width to that observed by Dkhil *et al* at (222) in the cubic phase. Subsequent neutron measurements of the (022) Bragg peak, taken with even higher q -resolution, also exhibit no splitting and mirror the results obtained at (111). In addition, the diffuse scattering and thermal expansion revealed by our neutron measurements differ considerably from those determined by x-ray diffraction. The implications of these results are significant. Combined with the results on PZN–8% PT and PZN obtained by Ohwada *et al* and Xu *et al* our results suggest that none of the relaxors in either the PMN– x PT or PZN– x PT family transforms to a rhombohedral phase for sufficiently low PT concentrations. Instead, they transform into Phase X.

2. Experimental details

All of the neutron scattering data presented here were obtained on the BT9 triple-axis spectrometer located at the NIST Center for Neutron Research (NCNR). The diffuse scattering near the (300) Bragg peak was measured at fixed incident and final neutron energies $E_i = E_f = 14.7$ meV ($\lambda = 2.36$ Å) using the (002) reflection of highly oriented pyrolytic graphite (HOPG) crystals as monochromator and analyser, and relatively relaxed horizontal beam collimations of $40'–46'–S–40'–80'$ ($S =$ sample). On the other hand, to maximize the instrumental sensitivity to subtle structural distortions and changes in lattice spacing, the BT9 spectrometer was operated in a special non-standard configuration in which a perfect Ge crystal was employed as analyser, and the d-spacings of the analyser and sample Bragg reflections were chosen to match one another as closely as possible. This latter condition yields a minimum in the instrumental longitudinal q -resolution [13, 14]. For the perovskite PMN–10% PT sample the (111) and (022) Bragg peak d-spacings (2.333 and 1.4287 Å, respectively) are well-matched with those for Ge (220) and (004) (2.000 and 1.4143 Å). Somewhat tighter horizontal beam collimations of $10'–46'–S–20'–40'$ were also used to improve the q -resolution further, but they did not result in an unreasonable reduction in intensity⁴. A lower neutron energy of 8.5 meV was used

⁴ Our choice of beam collimations were based on Monte Carlo intensity simulations performed by V Ghosh [14].

for measurements of the (111) Bragg peak, and resulted in a sharp q -resolution of 0.0018 rlu full-width at half-maximum (FWHM) ($1 \text{ rlu} = 2\pi/a = 1.5576 \text{ \AA}^{-1}$), while measurements of the (022) Bragg peak yielded a truly exceptional resolution of about 0.0010 rlu FWHM, owing to a more closely matched d -spacing condition between the sample and analyser.

A high quality single crystal of PMN–10% PT was obtained using a top-seeded solution growth technique [16]. The growth conditions were determined from the pseudo-binary phase diagram established for PMN and PbO. The crystal, which weighs 2.65 g (0.33 cm^3), is an irregular parallelepiped with dimensions $11.3 \times 9.2 \times 4.1 \text{ mm}$, the largest facets of which are oriented approximately normal to the cubic [100] direction. At 500 K the crystal mosaic measured at (200) is less than 0.06° FWHM. The crystal was mounted on a boron nitride post with the $[01\bar{1}]$ axis oriented vertically, giving access to reflections of the form (hll). The sample holder assembly was mounted inside the vacuum space of a high-temperature closed-cycle ^3He refrigerator that was then positioned and fixed onto the goniometer of the BT9 spectrometer.

3. The rhombohedral phase in PMN– x PT

In figure 1 we present the currently accepted phase diagram for PMN– x PT, which shows a cubic (C) to rhombohedral (R) phase transition for PbTiO_3 concentrations x less than $\approx 32\%$ [4, 5]. The solid circles represent measured values of T_c reported by various authors (see figure 4 of [8]), while the solid line is merely a guide to the eye. The lone data point for PMN ($x = 0$) corresponds to the first-order R-to-C phase transition that occurs at 213 K after first cooling in a field $E \geq 1.7 \text{ kV cm}^{-1}$ [15]. We use the notation \bar{C} shown by the arrow to denote the fact that PMN retains an average cubic structure below this temperature when zero-field cooled (ZFC). At higher PT concentrations, PMN– x PT exhibits a narrow region of monoclinic (M_c) phase discovered by Noheda *et al* [5] that lies next to the well-known morphotropic phase boundary (MPB) separating the M_c phase from the tetragonal (T) phase. The 10% PT concentration is indicated by the vertical dashed line in the phase diagram.

The inset to figure 1 shows the temperature dependence of the rhombohedral angle α (left-hand side scale), as well as that of the diffuse scattering (right-hand side scale) near the (300) Bragg peak (q not specified), for PMN–10% PT measured by Dkhil *et al* [10] using x-ray diffraction. The data for α are consistent with the occurrence of a first-order phase transition at 285 K, while the diffuse scattering, which is characterized by the authors as critical behaviour, displays a very broad peak centred at this same temperature.

4. Neutron diffuse scattering in PMN–10% PT

Neutron diffuse scattering results obtained on the single crystal of PMN–10% PT were obtained at the NCNR using relatively coarse horizontal beam collimations. These data, shown in figure 2 as a function of temperature, were measured along the $[011]$ direction near (300) at different values of the reduced wavevector q spanning the range $-0.30 \text{ rlu} \leq q \leq 0.30 \text{ rlu}$. A break in the slope of the diffuse scattering is evident for $q = -0.06 \text{ rlu}$ at a temperature near T_c (shown by the arrow). However, there is no evidence of the peak in intensity at T_c found by x-rays. Instead, the diffuse scattering intensity increases monotonically with decreasing temperature down to 50 K at all values of q studied. These data refute the idea that the diffuse scattering in PMN–10% PT is critical in nature. In fact, as shown in the inset to figure 2, the diffuse scattering is quite strong at 450 K, far above $T_c = 285 \text{ K}$. The diffuse scattering at this temperature appears as a very broad peak, with a maximum count rate of just under $10^3 \text{ counts min}^{-1}$, superimposed on top of the much narrower (300) Bragg peak which is roughly two orders of magnitude larger. In pure PMN, the diffuse scattering is known to

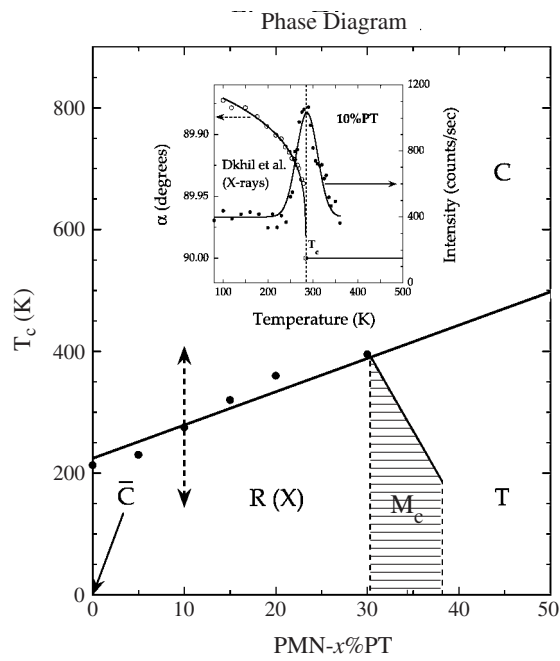


Figure 1. Currently accepted zero-field phase diagram of PMN-xPT [4, 5]. The inset shows the temperature dependence of the rhombohedral angle α and diffuse scattering measured with x-rays by Dkhil *et al* [10] on PMN-10% PT. Lines are guides to the eye.

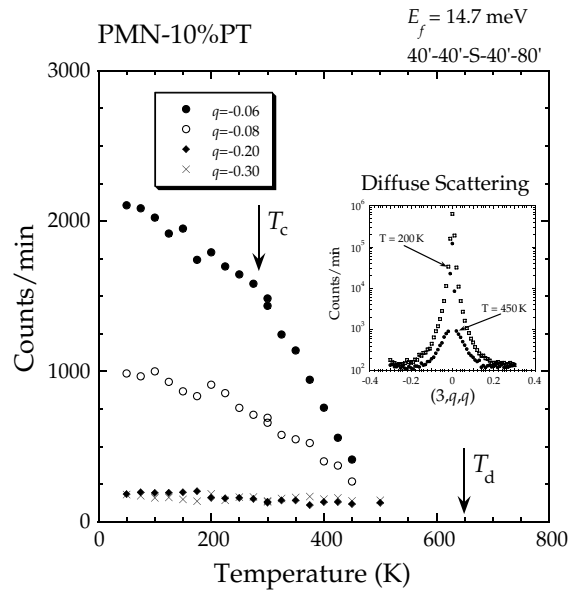


Figure 2. Neutron diffuse scattering intensity measured as a function of temperature at $\vec{Q} = (3, q, q)$ on a PMN-10% PT single crystal. The inset shows the full diffuse scattering profile measured along the [011] direction (transverse to \vec{Q}) at 200 and 450 K.

disappear near the Burns temperature $T_d = 600\text{--}650\text{ K}$ [17] above which polar nanoregions (PNR) no longer exist [18]. The corresponding approximate value of T_d for PMN–10% PT is shown by the arrow at 650 K.

5. Neutron Bragg diffraction with high q -resolution

Using the high q -resolution triple-axis neutron spectrometer configuration described earlier, radial and transverse q -profiles of the (111) Bragg peak of the PMN–10% PT crystal were measured down to 50 K. Two radial scans, one in the cubic phase at 325 K, and one in the rhombohedral phase at 100 K, are shown side-by-side in figure 3. Above these two scans are shown the corresponding x-ray scans from Dkhil *et al.* The horizontal scales for the x-ray data, which were measured at (222), have been reduced by a factor of 2 to allow for direct comparison to the neutron data, which were measured at (111). At high temperatures both x-ray and neutron data show the presence of a single resolution-limited peak, consistent with a cubic lattice. The horizontal bars represent the calculated BT9 instrumental q -resolution FWHM, and show that x-ray and neutron resolutions are comparable. At 80 K, the x-ray data show a clear splitting of the (222) peak. At roughly the same temperature, however, the neutron data show a single peak that is only slightly broader than resolution. These data contradict the finding that PMN–10% PT is rhombohedral below T_c .

To confirm this surprising behaviour, additional neutron measurements were made of the higher order (022) Bragg reflection using the same horizontal beam collimations of $10'\text{--}46'\text{--}S\text{--}10'\text{--}40'$, but with a higher incident and final neutron energy of 14.7 meV, which is required to reach the higher Q Bragg peak. This configuration provides an even better longitudinal q -resolution because of the substantially better matching between the sample (022) and Ge analyser (004) d-spacings. As was the case with the (111) Bragg peak, the (022) peak remains unsplit at all temperatures. These data are summarized in figure 4, and cover the temperature range from 10 to 650 K. In addition to the absence of any rhombohedral distortion down to 10 K, these data also show that the PMN–10% PT single crystal exhibits an anomalous thermal expansion between 10 and 400 K where the lattice constant changes by less than 0.001 Å. This behaviour contrasts sharply with that reported by Dkhil *et al.*, which is shown in the inset to figure 4. Above 400 K the rate of thermal expansion becomes extremely pronounced, and is roughly $1 \times 10^{-5}\text{ K}^{-1}$ (see dashed line), substantially larger than what is normally observed in oxide materials ($\sim 10^{-6}\text{ K}^{-1}$).

Two possibilities come to mind that could reconcile the neutron results with the x-ray results of Dkhil *et al.* and those of other x-ray studies. The first is that the PMN–10% PT single crystal in our study is a (dominantly) single-domain sample. In this case, no (111) or (022) peak splitting would be observed. However, Dkhil *et al.* report a first-order phase transition at $T_c = 285\text{ K}$, so one would still expect a jump in the lattice constant at T_c to either a larger or smaller d-spacing. But the data in figure 4 rule out this possibility because the variation of the PMN–10% PT lattice constant is monotonic and smooth with temperature across T_c , changing by less than 0.001 Å. In the x-ray case, the measured splitting at (222) corresponds to a difference in d-spacing of $\sim 0.012\text{ Å}$ at 80 K. In fact, it is highly unlikely for such a large crystal to exist as a single domain, particularly after having been zero-field cooled from high temperature. The second possibility is that a distribution of short-range ordered rhombohedral domain states is present that effectively smears out any Bragg peak splitting, so that only one (broader) peak is observed below T_c . This idea is easily refuted, however, since the FWHM q -width of the (111) Bragg peak measured with neutrons is *smaller* than the splitting observed with x-rays (refer to the horizontal bar in the upper left panel of figure 3). This is even more true for the (022) reflection, which is roughly two times narrower than the

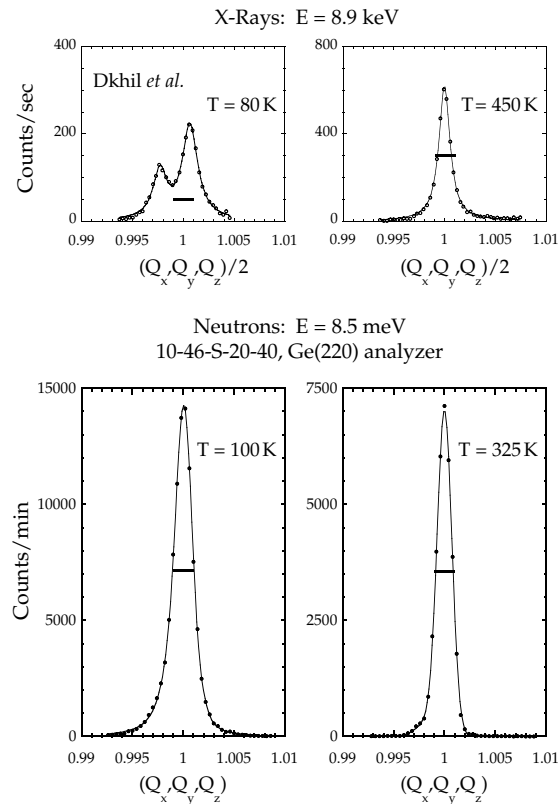


Figure 3. Comparison of x-ray measurements by Dkhil *et al* [10] at (222) (top) and our neutron measurements at (111) (bottom) on PMN-10% PT. The horizontal scale of the x-ray data has been reduced by a factor of two to allow direct comparison with the neutron (111) data. Solid bars indicate the BT9 instrumental q -resolution FWHM.

(111) reflection. Thus no such short-range ordered domains exist. And finally, neither of these possibilities could reconcile the discrepancies between the neutron and x-ray derived thermal expansions.

Our findings strongly support the picture in which *none* of the relaxors in the PMN- x PT family exhibit a rhombohedral phase in zero-field below T_c , at least for PT concentrations at or below 10%. The high-energy x-ray study of Xu *et al* demonstrates the presence of a $\approx 50 \mu\text{m}$ thick ($1 \mu\text{m} = 10^{-6} \text{m}$) outer layer in the closely related relaxor PZN that undergoes a rhombohedral distortion at low temperatures, while the interior volume of the crystal does not [12]. We believe this to be the case for PMN-10% PT as well. The presence of such an outer layer would reconcile the x-ray and neutron data shown in figure 3 since the 8.9 keV x-rays penetrate $\approx 10 \mu\text{m}$ into the sample whereas neutrons probe the entire crystal volume. It would also explain why the diffuse scattering peak observed with x-rays at T_c shown in figure 1 is absent when measured with neutrons (figure 2). Evidence for this outer layer is visible at the base of the 100 K neutron data shown in figure 3 where an asymmetric broadening is observed. A much weaker asymmetry is also visible in the neutron data shown in figure 3 at 325 K. Because neither x-rays nor neutrons see evidence of a rhombohedral distortion at this temperature, we believe this asymmetry results from the fact that the outer layer has a different d-spacing from that of the crystal bulk. In fact, K Colon *et al* have recently, demonstrated this

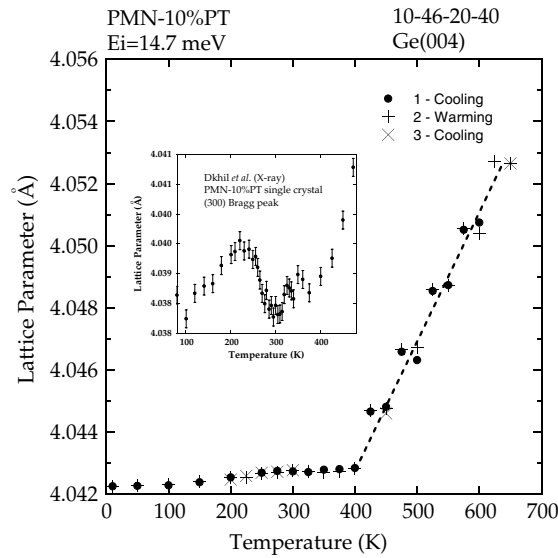


Figure 4. Thermal expansion for the PMN-10%PT single crystal sample determined from neutron measurements of the (220) Bragg peak. Inset shows the corresponding x-ray result, also for a single crystal sample of PMN-10%PT, based on measurements of the (300) Bragg peak taken from Dkhil *et al* [10].

to be the case of PMN at 300 K using neutron residual stress techniques [19]. While these data are insufficient to extract quantitative information about the thickness of the outer layer, they can be fitted to two Lorentzian peaks (representing the rhombohedral phase), and one Gaussian peak (for Phase X). The solid line shows a high quality of fit.

6. Discussion

In light of the neutron results of Ohwada *et al* [11] obtained on PZN-8% PT and Xu *et al* [12] on PZN we speculate that there is no bulk zero-field rhombohedral phase in PZN-*x*PT at sufficiently low PT concentrations either. We propose instead a new and universal phase diagram for both the PMN-*x*PT and PZN-*x*PT systems, as shown in figure 1, in which the rhombohedral phase is replaced by Phase X. Recent neutron studies by Xu *et al* on higher PT concentrations of PMN-*x*PT, which were motivated by our results, support this view [19]. This scenario is attractive not just because it reconciles the PMN anomaly, but also because it unifies the neutron scattering results of Wakimoto *et al* [20] that demonstrate the presence of a soft mode, and thus a ferroelectric polarization, below T_c in PMN, and also of Stock *et al* [21] who showed that PMN and PZN exhibit soft modes with identical temperature dependences below T_c .

Understanding the origin of this outer layer poses an interesting theoretical challenge, however we do not consider it to be of fundamental importance to the underlying properties of the relaxor compounds. Instead, we believe that the seminal question concerns the origin of Phase X, whose symmetry is unknown, and its relationship with the polar nanoregions. Starting from the diffuse scattering intensity measurements of Vakhrushev *et al* on PMN [22], Hirota *et al* proposed an entirely new model of the PNR [23]. When ionic displacements due to a normal ferroelectric distortion are determined from measurements of Bragg intensities

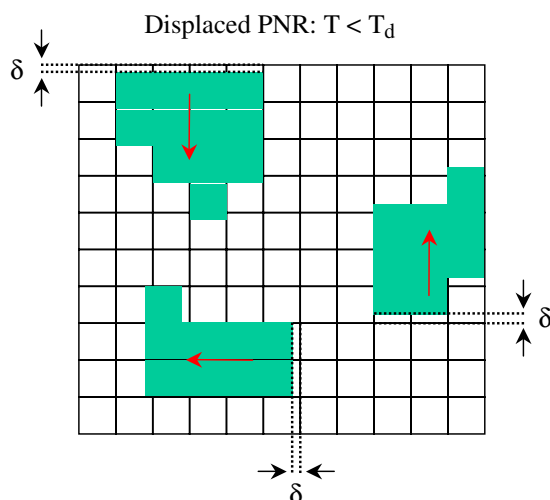


Figure 5. Schematic diagram of the polar nanoregions shown in green. White squares refer to the underlying perovskite cubic lattice. The PNR are displaced relative to the cubic lattice by a value of δ , shown by the dotted lines, in the direction of the PNR polar axis shown as red arrows.

below T_c , the point of reference (origin) for these displacements is arbitrary. Only the relative positions between the atoms are meaningful. But in the case of the diffuse scattering in PMN, which first appears several hundred degrees above T_c , the origin is not arbitrary because the surrounding lattice is still cubic. Following this reasoning, a simple inspection of the displacements given by Vakhrushev *et al* shows that the PNR centre-of-mass is shifted from that of surrounding cubic phase. An approximate representation of this shift is shown in figure 5. One logical way to interpret the PMN displacements is to view them as the sum of a centre-of-mass (COM) conserving component, and a scalar shift δ that is the same for all atoms. Using this approach Hirota *et al* demonstrated that the COM-conserving ionic displacements match the ionic motions associated with the soft TO mode, first observed above the Burns temperature T_d [24], thus lending strong experimental support to this interpretation. The uniform shift of the PNR has since been suggested to be the result of the coupling between the soft TO mode and the TA mode (first appreciated by Naberezhnov *et al* [17]). In this case, the soft coupled TO mode will necessarily carry an acoustic component that could explain the uniform shift [25, 26].

The essential point is that the uniform shift of the PNR, which is of the order of 60% of the Pb displacement, combined with their large ($\approx 30\text{--}50 \text{ \AA}^3$) size, makes the process of *melting* the PNR into the surrounding ferroelectric phase exceedingly difficult, and hence immensely slow. In this respect we believe it is the shift δ that stabilizes Phase X. While further studies are needed to characterize the PNR, and to determine the microscopic origin of the displacement δ , we believe that these ideas form the basis of an elegant and self-consistent model in which it is possible to understand the basic properties of these lead oxide relaxors.

Acknowledgments

We thank A Bokov, T Egami, K Hirota, K Ohwada, C Stock, S B Vakhrushev, D Vanderbilt, S Wakimoto and G Xu for stimulating discussions. We acknowledge financial support from the US Department of Energy under contract no DE-AC02-98CH10886, and the Office of

Naval Research, grant no N00014-99-1-0738. We also acknowledge the US Department of Commerce, NIST Center for Neutron Research, for providing the neutron scattering facilities used in this study.

References

- [1] Bonneau P, Garnier P, Husson E and Morell A 1989 *Mater. Res. Bull.* **24** 201
Bonneau P, Garnier P, Calvarin G, Husson E, Gavarrri J R, Hewat A W and Morell A 1991 *J. Solid State Chem.* **91** 350
- [2] de Mathan N, Husson E, Calvarin G, Gavarrri J R, Hewat A W and Morell A 1991 *J. Phys.: Condens. Matter* **3** 8159
- [3] Ye Z-G 1998 *Key Eng. Materials* **155–156** 81
- [4] Choi S W, Shrout T R, Jang S J and Bhalla A S 1989 *Ferroelectrics* **100** 29
- [5] Noheda B, Cox D E, Shirane G, Gao J and Ye Z-G 2002 *Phys. Rev. B* **66** 054104
- [6] Kuwata J, Uchino K and Nomura S 1981 *Ferroelectrics* **37** 579
- [7] La-Orauttapong D, Noheda B, Ye Z-G, Gehring P M, Toulouse J, Cox D E and Shirane G 2002 *Phys. Rev. B* **65** 144101
- [8] Ye Z-G, Bing Y, Gao J, Bokov A A, Stephens P, Noheda B and Shirane G 2003 *Phys. Rev. B* **67** 104104
- [9] Lebon A, Dammak H, Calvarin G and Ahmedou I O 2002 *J. Phys.: Condens. Matter* **14** 7035
- [10] Dkhil B, Kiat J M, Calvarin G, Baldinozzi G, Vakhrushev S B and Suard E 2001 *Phys. Rev. B* **65** 024104
- [11] Ohwada K, Hirota K, Rehrig P W, Fujii Y and Shirane G 2003 *Phys. Rev. B* **67** 094111
- [12] Xu G, Zhong Z, Bing Y, Ye Z-G, Stock C and Shirane G 2003 *Phys. Rev. B* **67** 104102
- [13] Lorenzo J E *et al* 1994 *Phys. Rev. B* **50** 1278
- [14] Xu G, Gehring P M, Ghosh V J and Shirane G 2004 *Acta Crystallogr. A*, submitted (*Preprint cond-mat/0401439*)
- [15] Vakhrushev S B, Naberezhnov A A, Okuneva N M and Savenko B N 1998 *Phys. Solid State* **40** 1728
- [16] Chen W and Ye Z-G 1990 unpublished
Ye Z-G, Tissot P and Schmid H 1990 *Mater. Res. Bull.* **25** 739
- [17] Naberezhnov A, Vakhrushev S B, Dornier B and Moudden H 1999 *Eur. Phys. J. B* **11** 13
- [18] Burns G and Dacol F H 1983 *Solid State Commun.* **48** 853
Burns G and Dacol F H 1983 *Phys. Rev. B* **28** 2527
Colon K, Luo H, Viehland D, Li J F, Whan T, Fox J H, Stock C and Shirane G 2004 (*Preprint cond-mat/0407609*)
- [19] Xu G, Viehland D, Li J F, Gehring P M and Shirane G 2003 *Phys. Rev. B* **68** 212410
- [20] Wakimoto S, Stock C, Birgeneau R J, Ye Z-G, Chen W, Buyers W J L, Gehring P M and Shirane G 2002 *Phys. Rev. B* **65** 172105
- [21] Stock C, Birgeneau R J, Wakimoto S, Gardner J S, Chen W, Ye Z-G and Shirane G 2003 *Preprint cond-mat/0301132*
- [22] Vakhrushev S B, Naberezhnov A A, Okuneva N M and Savenko B N 1995 *Phys. Solid State* **37** 1993
- [23] Hirota K, Ye Z-G, Wakimoto S, Gehring P M and Shirane G 2002 *Phys. Rev. B* **65** 104105
- [24] Gehring P M, Wakimoto S, Ye Z-G and Shirane G 2001 *Phys. Rev. Lett.* **87** 277601
- [25] Yamada Y and Takakura T 2002 *Preprint cond-mat/0209573*
- [26] Wakimoto S, Stock C, Ye Z-G, Chen W, Gehring P M and Shirane G 2002 *Phys. Rev. B* **66** 224102